

# Robust Infrared-Shielding Coating Films Prepared Using Perhydropolysilazane and Hydrophobized Indium Tin Oxide Nanoparticles with Tuned Surface Plasmon Resonance

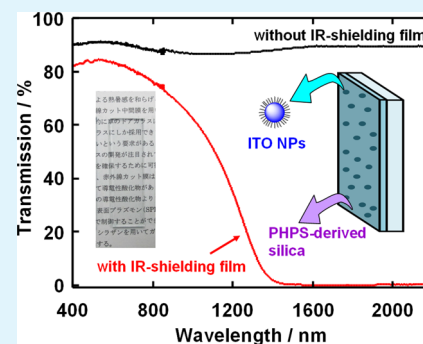
Kiyofumi Katagiri,\* Ryuichi Takabatake, and Kei Inumaru

Department of Applied Chemistry, Graduate School of Engineering, Hiroshima University, 1-4-1, Kagamiyama, Higashi-Hiroshima, Hiroshima 739-8527, Japan

## Supporting Information

**ABSTRACT:** Robust infrared (IR)-shielding coating films were prepared by dispersing indium tin oxide (ITO) nanoparticles (NPs) in a silica matrix. Hydrophobized ITO NPs were synthesized via a liquid phase process. The surface plasmon resonance (SPR) absorption of the ITO NPs could be tuned by varying the concentration of Sn doping from 3 to 30 mol %. The shortest SPR wavelength and strongest SPR absorption were obtained for the ITO NPs doped with 10% Sn because they possessed the highest electron carrier density. Coating films composed of a continuous silica matrix homogeneously dispersed with ITO NPs were obtained using perhydropolysilazane (PHPS) as a precursor. PHPS was completely converted to silica by exposure to the vapor from aqueous ammonia at 50 °C. The prepared coating films can efficiently shield IR radiation even though they are more than 80% transparent in the visible range. The coating film with the greatest IR-shielding ability completely blocked IR light at wavelengths longer than 1400 nm. The pencil hardness of this coating film was 9H at a load of 750 g, which is sufficiently robust for applications such as automotive glass.

**KEYWORDS:** indium tin oxide, perhydropolysilazane, nanoparticles, coating films, infrared shielding



## INTRODUCTION

Transparent conducting oxides (TCOs) are widely used as transparent conducting coating films for optoelectronic devices, including electroluminescence and liquid crystal displays, solar cells, and touch screens.<sup>1–3</sup> Typically, n-type semiconductors such as indium tin oxide (ITO) and fluorine- or antimony-doped tin dioxide are employed as TCOs in these applications.<sup>4–6</sup> With the growing interest in energy conservation, recent research using TCOs has focused not only on optoelectronic devices but also on photoprotective materials.<sup>7–9</sup> TCOs exhibit surface plasmon resonance (SPR) frequencies in the near-infrared (NIR) region because TCOs have charge carrier densities lower than those of typical noble metals such as Au, Ag, and Pt.<sup>10–13</sup> Therefore, TCOs allow a high level of transmission of visible light and possess the ability to shield infrared (IR) radiation. TCO-based photoprotective materials are promising for IR-shielding windows in automobiles and buildings, contact lenses, and heat mirrors.<sup>14–17</sup> IR-shielding glass is an attractive option for automobiles because it can be used as a thermal insulator.<sup>18</sup> Via the shielding of IR radiation from the sun, the increase in temperature inside an automotive cabin is suppressed. As a result, the use of air conditioning in automobiles can be reduced and fuel efficiency correspondingly increased. In addition, IR-shielding glass can improve the comfort of passengers because the time to cool the cabin should be shortened and skin burn feelings can be relieved by shielding direct solar radiation. ITO is a promising

candidate as a photoprotective material because of its remarkable combination of high transparency in the visible region and high IR reflectivity.<sup>7,9,19,20</sup> In most cases, ITO is used as coating films prepared by the sol–gel method,<sup>21,22</sup> chemical vapor deposition,<sup>23</sup> pulsed laser deposition,<sup>24</sup> or magnetron sputtering.<sup>25,26</sup> However, these techniques involve high-temperature and/or vacuum treatment, which increase the rate of consumption of energy and the cost of equipment. In addition, continuous ITO coating is inappropriate for automotive windows because it also shields radio waves and causes cellular phones to have poor reception in the cabins of vehicles.<sup>18</sup> To overcome these issues, a new class of nanostructured materials, e.g., polymer–ITO nanoparticle (NP) composites, has been developed by various groups.<sup>27–31</sup> These nanocomposites are composed of a continuous transparent polymer matrix homogeneously dispersed with ITO NPs. Isolation of ITO NPs allows radio wave permeability while maintaining strong IR-shielding ability. However, the robustness of these nanocomposites reported to date is insufficient for automotive glass, especially as side windows because they are raised and lowered repetitively by electric window lifts.

Received: July 25, 2013

Accepted: September 11, 2013

Published: September 11, 2013

In this study, we developed robust IR-shielding coating films composed of a silica matrix homogeneously dispersed with ITO NPs. To tune their SPR absorption and control the electron carrier density in ITO, the ITO NPs were doped with different concentrations of Sn.<sup>10,11</sup> Coating films containing the ITO NPs with the shortest SPR wavelength and strongest SPR absorption were investigated. The ITO NPs were prepared as organically modified NPs using a liquid phase process. The agglomeration of ITO NPs could be suppressed even in dispersions with high concentrations because they were coated with hydrophobic organic chains. This allowed a high concentration of ITO NPs to be incorporated into film matrices. Simply blending hydrophobized ITO NPs with sol-gel-derived silica usually results in agglomeration of the NPs within the silica matrices and loss of optical transparency because of intense light scattering by the agglomerated NPs. Here, we used perhydropolysilazane (PHPS) as a precursor for the silica matrix.<sup>32–35</sup> It is possible to mix PHPS and hydrophobized ITO NPs with high concentrations because PHPS is soluble in various nonpolar organic solvents. In addition, PHPS can be transformed into silica with high density and robustness using a low-temperature process (<100 °C). Recently, Kozuka et al. reported that PHPS-to-silica conversion was achieved by exposing PHPS coating films to the vapor from aqueous ammonia at room temperature.<sup>33,34</sup> They also reported that homogeneous organic–inorganic hybrid coatings composed of poly(methyl methacrylate) (PMMA) and silica can be prepared using PHPS.<sup>35</sup> It is noteworthy that hydrophilic silica and hydrophobic PMMA did not undergo phase separation even after the conversion of PHPS to silica. Therefore, we expect that agglomeration of the hydrophobized ITO NPs within the silica matrices is suppressed by using PHPS as the source of silica. To the best of our knowledge, the preparation of IR-shielding coating films using a combination of hydrophobized ITO NPs and PHPS has not been reported. To optimize the IR-shielding ability of the silica–ITO NP coatings, the effects of Sn doping concentration, the concentration of ITO NPs in the coating solution, and the number of spin-coated layers were investigated in detail. We also studied the robustness of the coating film with the strongest IR-shielding ability.

## EXPERIMENTAL SECTION

**Materials.** Indium(III) acetate, oleylamine, and dioctyl ether were purchased from Sigma-Aldrich. Ethanol, hexane, and tin(II) octylate were obtained from Nacalai Tesque, Inc. Aqueous ammonia [28% (w/w)] and *n*-octanoic acid were purchased from Kishida Chemical Co., Ltd. A dibutyl ether solution of PHPS [20% (w/w), NN120-20] was obtained from Sanwa Kagaku Co. All reagents were used as received without further purification. The water used in all experiments was deionized with a Millipore Milli-Q system.

**Preparation of Hydrophobized ITO NPs.** Indium(III) acetate was mixed with dioctyl ether (20 mL) in a three-neck round-bottom flask. Tin(II) octylate, *n*-octanoic acid (7.2 mmol), and oleylamine (20 mmol) were added to the mixture and stirred for 80 °C under vacuum for 30 min. The total number of moles of indium(III) acetate and tin(II) octylate was 2.4 mmol. The solution was then heated at 150 °C for 1 h under a N<sub>2</sub> atmosphere and stirred for a further 2 h at 280 °C to obtain ITO NPs. Ethanol was added to the obtained solution to aggregate the ITO NPs. The aggregated ITO NPs were collected by centrifugation and then redispersed in hexane. ITO NPs with different mole percentages of Sn [3, 5, 10, 20, and 30%, where % =  $[\text{Sn}]/([\text{Sn}] + [\text{In}]) \times 100$ ] were synthesized in this manner.

**Preparation of IR-Shielding Coating Films Using PHPS and Hydrophobized ITO NPs.** Soda-lime-silica glass substrates were used

to prepare IR-shielding coating films. The substrates were cleaned by ultrasonication in ethanol for 30 min. Identical volumes of an as-received dibutyl ether solution of PHPS and hexane dispersion of hydrophobized ITO NPs were mixed to form coating solutions for the IR-shielding coating films. ITO NPs with different mole percentages of Sn were used in the coating solutions. The concentration of ITO NPs in the coating solution was also varied (25, 50, and 100 mg/mL). Glass substrates used for substrates were cleaned using the RCA protocol [i.e., by immersion in a 5:1:1 H<sub>2</sub>O/aqueous H<sub>2</sub>O<sub>2</sub>/aqueous NH<sub>4</sub>OH (v/v/v) mixture for 10 min at 70 °C] and then rinsed with deionized water. Coating films were fabricated on glass substrates by spin-coating at 1500 rpm. Two, six, or 10 spin-coated layers were formed. Immediately after spin-coating had been conducted, the substrates were exposed to the vapor from aqueous ammonia at 50 °C for 24 h in the following manner. A mixture of aqueous ammonia [20 mL, 28% (w/w)] and deionized water (10 mL) was placed in a container. The glass substrates with coating films were positioned vertically in the container. The top of the container was covered with plastic wrap perforated multiple times with a needle. For comparison, coatings were also formed using a solution without ITO NPs (PHPS only). In addition, coatings were also prepared using Si wafers for the Fourier transform infrared (FT-IR) measurements. These coatings were fabricated in the same manner that was used on glass substrates.

**Characterization.** Structural information about ITO NPs was obtained by X-ray diffraction (XRD) (D8 Advance, Bruker AXS) using Cu K $\alpha$  radiation. Transmission electron microscopy (TEM) images were captured with a JEOL JEM-2010 microscope operating at 200 kV. Samples were prepared by depositing a droplet of each dispersion on carbon-coated copper grids covered with elastic carbon films and drying in air overnight. Scanning electron microscopy (SEM) images were captured with a Hitachi S-4800 microscope. FT-IR spectra were collected with a JASCO FT/IR-4200 spectrometer fitted with a Universal ATR polarization accessory and recorded over the range of 2500–400 cm<sup>-1</sup>. UV–vis–NIR spectra were measured by a spectrophotometer (PerkinElmer Lambda 900) for both dispersions of ITO NPs and IR-shielding coating films. The pencil hardness of the coating films was measured according to JIS-K5600-5-4 using a pencil scratch hardness tester (KT-VF2380, COTEC Co.).

## RESULTS AND DISCUSSION

Hydrophobized ITO NPs with different mole percentages of Sn (3, 5, 10, 20, and 30%) were synthesized by a liquid phase process using dioctyl ether and *n*-octanoic acid. The XRD patterns obtained for the ITO NPs after the hydrothermal process are shown in Figure 1. Peaks that can be assigned to the (2 1 1), (2 2 2), (4 0 0), (4 3 1), (4 4 0), and (6 2 2) planes of the crystal faces of the cubic structure of In<sub>2</sub>O<sub>3</sub> (ICDD PDF No. 06-0416) were observed for the ITO NPs with different

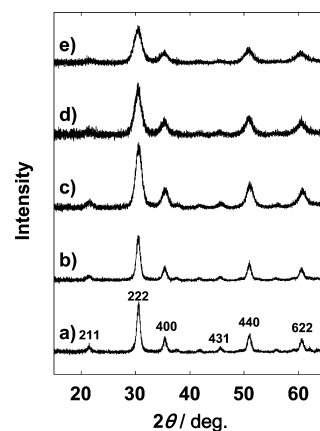


**Figure 1.** XRD patterns of hydrophobized ITO NPs doped with (a) 3, (b) 5, (c) 10, (d) 20, and (e) 30% Sn.

mole percentages of Sn (3–30%). No peaks from crystalline SnO or SnO<sub>2</sub> were detected, indicating that the In atoms were replaced by Sn atoms to form highly crystalline ITO NPs without the formation of tin oxides. These results also reveal that the content of Sn in the ITO NPs could be controlled from 3 to 30%. The strong diffraction peaks indicated that the as-prepared ITO NPs were highly crystalline. However, the full widths at half-maximum (FWHMs) of the diffraction peaks were relatively broad because of the formation of nanoscale crystals of ITO. The average crystallite sizes evaluated from the FWHM of the (2 2 2) diffraction peak of the ITO NPs containing 3, 5, 10, 20, and 30% Sn using Scherrer's equation were 10.7, 8.8, 5.7, 5.6, and 4.9 nm, respectively.

The morphology and size of the ITO NPs were investigated by TEM observation, as presented in Figure 2. These images

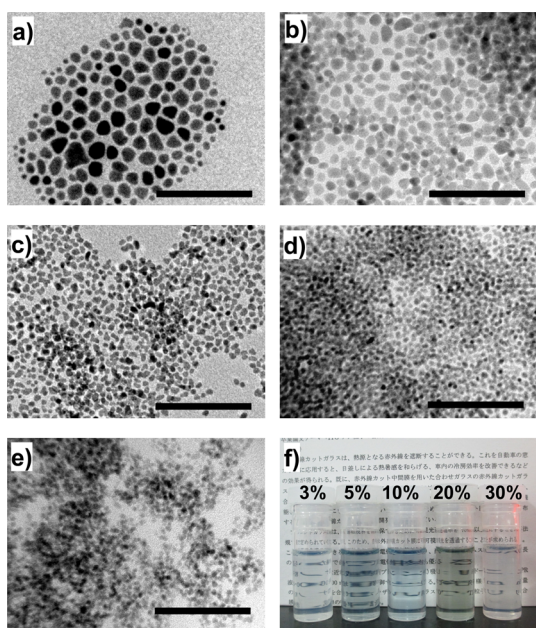


**Figure 2.** TEM images of hydrophobized ITO NPs doped with (a) 3, (b) 5, (c) 10, (d) 20, and (e) 30% Sn. The scale bars are 100 nm. (f) Photographic image of dispersions of ITO NPs in hexane. The concentration of ITO NPs in dispersions was 200 mg/mL.

revealed that the ITO NPs were well dispersed with nearly spherical shapes. The mean diameters of ITO NPs measured from the TEM images were 5–10 nm and decreased with the increasing mole percentage of Sn. This tendency is in good agreement with that found from XRD analysis. A photographic image of a dispersion of ITO NPs in hexane is shown in Figure 2f. Transparent dispersions were obtained for ITO NPs with different Sn contents. These dispersions were quite stable under ambient conditions for several months without any precipitation, aggregation, or gelation. These results indicate that the ITO NPs prepared here were hydrophobic because their surfaces were capped with the organic tails of *n*-octanoic acid. Consequently, these particles readily dispersed in hydrophobic organic solvents such as hexane.

FT-IR spectra were measured to reveal the interaction between the organic molecules and ITO NP surface. Figure 3 shows FT-IR spectra of ITO NPs prepared using *n*-octanoic acid and *n*-octanoic acid itself. Bands in the 2840–2970 cm<sup>-1</sup> region are attributed to the symmetric and asymmetric stretching of CH<sub>2</sub> groups and the terminal CH<sub>3</sub> group. The

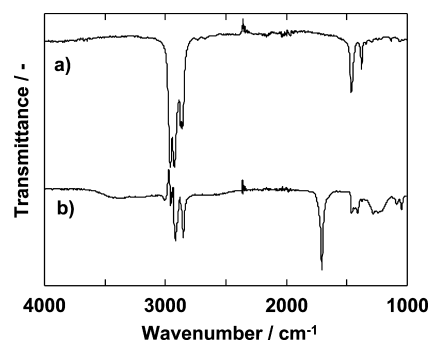


**Figure 3.** FT-IR spectra of (a) ITO NPs prepared using *n*-octanoic acid and (b) *n*-octanoic acid itself.

strong peak at 1707 cm<sup>-1</sup> in the spectrum of *n*-octanoic acid, which is associated with the stretching vibration of the free C=O group, is almost absent in the spectrum of ITO NPs. In contrast, two characteristic bands at 1465 and 1378 cm<sup>-1</sup> are apparent in the spectrum of the ITO NPs that are consistent with COO<sup>-</sup> asymmetric and symmetric stretching vibrations, respectively, of carboxylate anions complexed with surface metal centers of the ITO NPs.<sup>36,37</sup> This suggests chemical bonds formed between the nanocrystalline surface of ITO and organic ligand molecules, which promote dispersion of ITO NPs in nonpolar organic solvents. UV-vis-NIR spectra of ITO NPs doped with different amounts of Sn are presented in Figure 4. The ITO NPs exhibited an interband transition at ~400 nm and absorbed weakly in the red region. Therefore, hexane dispersions of the ITO NPs were light blue (Figure 2f). In the NIR region, the ITO NPs showed clear SPR absorbance from 1600 nm. The position of SPR absorption gradually shifted from >2200 to 1794 nm as the content of Sn increased from 3 to 10% (Figure 4a). However, further doping of ITO

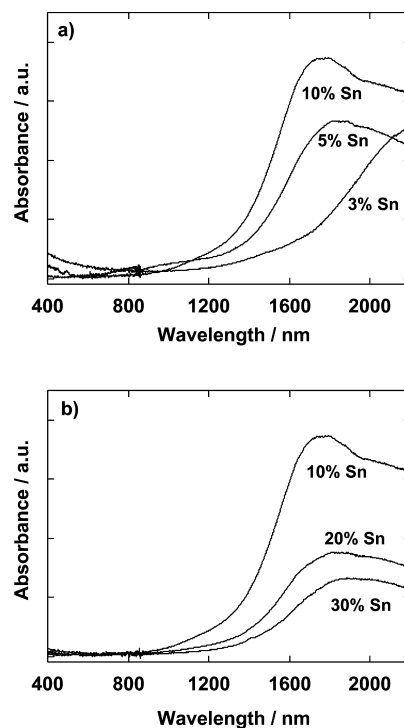


**Figure 4.** UV-vis-NIR spectra of ITO NPs doped with (a) 3–10% Sn and (b) 10–30% Sn.



with Sn caused the peak to shift to longer wavelengths; it shifted from 1811 to 1897 nm as the Sn content increased from 20 to 30% (Figure 4b). NPs with shorter SPR wavelengths have higher densities of free electrons. Replacement of In sites with Sn atoms produces free electrons.<sup>38</sup> Here, increasing the percentage of Sn up to ~10% causes the electron density to increase. However, further doping with Sn (>10%) causes the electron density to decrease because Sn<sup>4+</sup> acts as a carrier trapping site when the concentration of Sn is high.<sup>38</sup> As a result, ITO NPs doped with 10% Sn show the shortest SPR wavelength and strongest absorption for the Sn doping range of 3–30%. It is known that the maximal carrier concentration and minimal resistivity are obtained when a thin film of ITO is doped with ~10% Sn,<sup>21,38,39</sup> so our results are in good agreement with those in the literature.

The ITO NPs prepared here can be dispersed in nonpolar organic solvents such as hexane. We used PHPS as a precursor for silica because it is also soluble in various organic solvents. A commercially available PHPS solution (solvent of dibutyl ether) could be mixed with hexane dispersions of the ITO NPs. Homogeneous mixtures without any aggregation, gelation, or phase separation were easily obtained and then used as coating solutions. Coating films were prepared by spin-coating these mixtures on glass substrates. The substrates used for coating were cleaned using the RCA protocol. The surface of substrates was hydrophilic because of the presence of silanol groups. This cleaning process is important for making strong adhesion between substrates and films after PHPS-to-silica conversion. The dewetting phenomena during the spin-coating process were not observed even when hydrophobic coating solutions were employed. SEM observation revealed that the surface of coating films was very smooth (Figure S1 of the Supporting Information). The as-deposited films were then exposed to the vapor from aqueous ammonia to convert PHPS to silica. Figure 5 shows FT-IR spectra of coating films measured before and

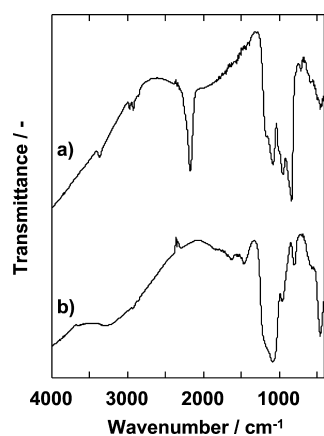


**Figure 5.** FT-IR spectra of coating films prepared using PHPS and ITO NPs (a) before and (b) immediately after exposure to the vapor from aqueous ammonia.

after exposure to the vapor from aqueous ammonia. When the films were exposed to the ammonia vapor, peaks attributed to the Si–H stretching vibration (2174 cm<sup>-1</sup>), the N–H bending vibration in Si–NH–Si species (1166 cm<sup>-1</sup>), the Si–H deformation vibration (948 cm<sup>-1</sup>), and the Si–H wag vibration (834 cm<sup>-1</sup>) disappeared.<sup>34</sup> Conversely, the bands assigned to Si–O–Si asymmetric stretching longitudinal and transverse optical modes (1220 and 1081 cm<sup>-1</sup>, respectively) and the Si–

O–Si rocking mode (455 cm<sup>-1</sup>) appeared after exposure to the vapor. These results indicate that PHPS was completely converted to silica by exposure to the vapor from aqueous ammonia. Peaks assigned to symmetric and asymmetric stretching of CH<sub>2</sub> groups and the terminal CH<sub>3</sub> group (2840–2970 cm<sup>-1</sup>) were found in spectra measured both before and after exposure. These peaks were derived from alkyl groups on the surface of the ITO NPs. Therefore, ITO NPs remained well dispersed in the silica matrix.

It is well known that SPR frequency is affected by the refractive index of the surrounding medium.<sup>40,41</sup> From Mie theory, a plasmon material that is surrounded by a medium with a higher refractive index is expected to have a lower SPR frequency. Therefore, ITO NPs with different mole percentages of Sn were used in coating films, and their IR-shielding abilities were compared. Figure 6 presents the UV–vis–NIR trans-

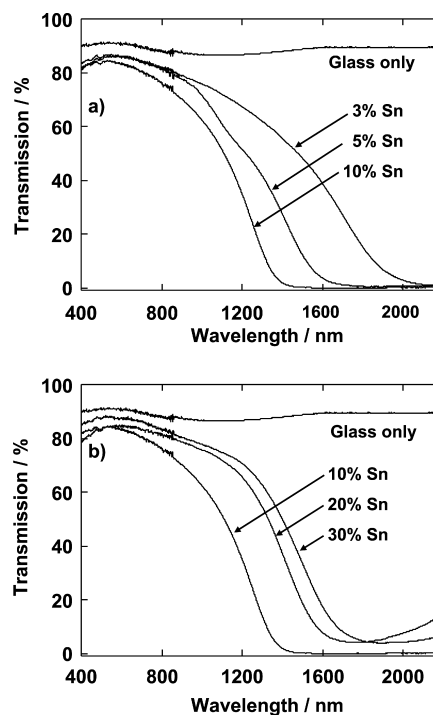


**Figure 6.** UV–vis–NIR transmission spectra of coating films formed with PHPS-derived silica and ITO NPs doped with (a) 3–10% Sn and (b) 10–30% Sn on glass substrates.

mission spectra of glass substrates with coating films prepared using ITO NPs with various Sn contents. The concentration of ITO NPs was fixed at 50 mg/mL. Spin-coating was performed 10 times for each coating film. For comparison, a spectrum of the uncoated substrate is also shown in Figure 6. The glass substrate was ~90% transparent over the whole range of 400–2200 nm, so the glass substrate cannot reflect NIR radiation. All of the substrates with coating films formed from PHPS-derived silica and ITO NPs with different contents of Sn remained more than 80% transparent in the visible range (400–800 nm). Importantly, all of the substrates with coating films showed low transmittance in the NIR range (800–2200 nm). The IR transmission cutoff wavelength of the coatings shifted to shorter wavelengths with an increasing content of Sn in the ITO NPs up to 10% (Figure 6a). However, further doping of Sn (>10%) caused the IR transmission cutoff wavelength to shift to a longer wavelength (Figure 6b). This tendency is

similar to the spectra of the as-synthesized ITO NPs in solution. Figure 7 shows photographs of glass substrates with

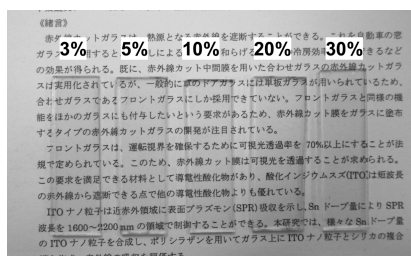


**Figure 7.** Photographic image of glass substrates with coating films formed with PHPS-derived silica and ITO NPs doped with various amounts of Sn.

coating films prepared using ITO NPs with various Sn contents. The coating films are highly transparent, and no visible clouding is observed. The high optical clarity of the prepared composites can be attributed to the good dispersion of the hydrophobized ITO NPs within the PHPS-derived silica matrix, which minimizes the scattering loss. TEM observation showed that the ITO NPs were considerably smaller than the wavelengths of visible light and did not form large agglomerates that could cause light scattering. Therefore, optical scattering by the coating films was suppressed. It is noteworthy that formation of agglomerates of hydrophobized ITO NPs was prevented even after conversion of the matrix from hydrophobic PHPS to hydrophilic silica.

Next, the effects of the concentration of ITO NPs in the coating films and the number of spin-coated layers on the properties of the film coatings were investigated. ITO NPs doped with 10% Sn were used in these experiments. Figure 8a

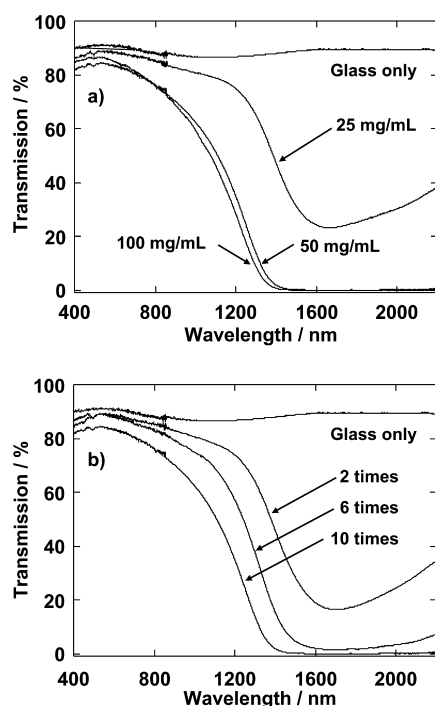


**Figure 8.** UV-vis-NIR transmission spectra of coating films formed with PHPS-derived silica and ITO NPs on glass substrates investigating the variation in (a) the concentration of ITO NPs in the coating solution and (b) the number of spin-coated layers.

presents the UV-vis-NIR transmission spectra of glass substrates with coating films prepared from coating solutions containing various concentrations of ITO NPs. Spin-coating was performed 10 times for each sample. The IR-shielding ability of the coatings films improved with the concentration of ITO NPs in the coating solution from 25 to 50 mg/mL. However, a higher concentration of ITO NPs of 100 mg/mL did not improve the IR-shielding ability. In addition, the film prepared using a coating solution containing 100 mg/mL ITO NPs was bluer than that prepared using the coating solution with 50 mg/mL ITO NPs (Figure S2 of the Supporting Information). Therefore, a concentration of ITO NPs of 50 mg/mL should be sufficient to produce a high NIR shielding efficiency.

UV-vis-NIR transmission spectra of glass substrates with coating films with different numbers of spin-coated layers are depicted in Figure 8b. The concentration of ITO NPs was fixed at 50 mg/mL. The films contained two, six, or 10 spin-coated layers. The IR-shielding ability of the coating films improved with the number of spin-coated layers. However, the transparency in the visible range decreased slightly upon increasing the number of spin-coated layers from six to 10, although the sample with 10 spin-coated layers remained more than 80% transparent in the visible range. The coatings were sufficiently transparent, and no visible clouding was observed (Figure S3 of the Supporting Information). Further increasing the number of spin-coated layers in the films caused their transparency in the visible range to decrease markedly. Usually, laws require more than 80% transparency in the visible range for automotive glass. Therefore, the optimal number of spin-coated layers should be 10 in this system. The coating films prepared using the optimal conditions (ITO NPs doped with 10% Sn, concentration of ITO NPs of 50 mg/mL, and 10 spin-coated layers) can completely shield IR light at wavelengths longer than 1400 nm. Using this method, the IR-shielding ability of the obtained film is comparable with better results reported previously.<sup>27–31</sup> In previous work, the coating films have an obvious greenish color, although they showed nearly 100% IR-shielding efficiency at wavelengths longer than 1500 nm.<sup>30</sup>

To estimate the robustness of the coating films, they were subjected to the pencil hardness test. Their pencil hardness was measured according to JIS-K5600-5-4 (load of 750 g, pencil angle of 45°). The coating film prepared using PHPS and ITO NPs (10% Sn, concentration of ITO NPs of 50 mg/mL, and 10 spin-coated layers) had a pencil hardness as low as 6H. The pencil hardness of the coating films increased to more than 9H after conversion of PHPS to silica. This result indicates that the coating films prepared with ITO NPs have hardness comparable to that of pure PHPS-derived silica films, i.e., that without ITO NPs.<sup>35</sup> This value is sufficiently high for application as automotive glass. The thickness of the coating film determined by cross-sectional scanning electron microscope (SEM) observation was ~750 nm (Figure S4 of the Supporting Information). The SEM image also shows that the coating film possesses a smooth surface and dense microstructure. Previously, Kumon et al.<sup>42</sup> prepared IR-shielding coating films using sol-gel-derived organically modified silica and ITO NPs. Their films required a thickness of >1.0 μm and heat treatment at 160 °C to achieve a pencil hardness of 9H. Moreover, their films were 10% transparent at 1500 nm. Other reported IR-shielding coatings were not robust (i.e., pencil hardness of 9H) because organic polymers were used as matrices. Comparison with previous reports reveals that the

performance of the coating films developed here is much better in terms of both IR-shielding ability and robustness.

## CONCLUSIONS

Hydrophobized ITO NPs <10 nm in size were successfully prepared by a liquid phase process. The SPR absorption of the ITO NPs could be tuned by varying the concentration of the Sn dopant. The shortest SPR wavelength and strongest SPR absorption were obtained for the ITO NPs doped with 10% Sn. This was attributed to these NPs possessing the highest electron carrier density among those prepared. Homogeneous coating films formed of silica matrices dispersed with ITO NPs were obtained using PHPS as a precursor for silica. PHPS was completely converted to silica by exposure to the vapor from aqueous ammonia. The prepared coating films were more than 80% transparent in the visible range because agglomeration of the ITO NPs within the silica matrices was suppressed. The coating films demonstrate low transmittance of NIR light. The strongest IR-shielding ability was obtained using ITO NPs with 10% Sn, a concentration of ITO NPs of 50 mg/mL, and 10 layers spin-coated on the substrate. The coating film formed under these conditions can completely block IR light at wavelengths longer than 1400 nm. The pencil hardness of this coating film was 9H at a load of 750 g, which is comparable to that of pure silica films prepared by the sol-gel method with high-temperature heat treatment. This robustness is sufficient for application as automotive glass.

## ASSOCIATED CONTENT

### Supporting Information

SEM image of the surface of the coating film formed with PHPS and ITO NPs and photographic images and cross-sectional SEM image of glass substrates with coating films formed with PHPS-derived silica and ITO NPs. This material is available free of charge via the Internet at <http://pubs.acs.org>.

## AUTHOR INFORMATION

### Corresponding Author

\*E-mail: [kktgr@hiroshima-u.ac.jp](mailto:kktgr@hiroshima-u.ac.jp)

### Notes

The authors declare no competing financial interest.

## ACKNOWLEDGMENTS

This work was financially supported by Grants-in-Aid for Scientific Research (20107011) in the Innovative Area "Fusion Materials" (Area 2206, <http://www.fusion-materials.org/en/>) from the Ministry of Education, Culture, Sports, Science and Technology (MEXT).

## REFERENCES

- (1) Ginley, D. S.; Bright, C. *MRS Bull.* **2000**, *25*, 15.
- (2) Ohta, H.; Hosono, H. *Mater. Today* **2004**, *7*, 42.
- (3) Liu, H.; Avrutin, V.; Izyumskaya, N.; Özgür, Ü.; Morkoç, H. *Superlattices Microstruct.* **2010**, *48*, 458.
- (4) Hartnagel, H. L.; Dawar, A. L.; Jain, A. K.; Jagdish, C. *Semiconducting Transparent Thin Films*; IOP Publishing Ltd.: Bristol, U.K., 1995.
- (5) Bisht, H.; Eun, H.-T.; Mehrkens, A.; Aegerter, M. A. *Thin Solid Films* **1999**, *351*, 109.
- (6) Kawashima, T.; Matsui, H.; Tanabe, N. *Thin Solid Films* **2003**, *445*, 241.
- (7) Usui, H.; Sasaki, T.; Koshizaki, N. *J. Phys. Chem. B* **2006**, *110*, 12890.
- (8) Meng, L.-J.; Gao, J.; dos Santos, M. P.; Wang, X.; Wang, T. *Thin Solid Films* **2008**, *516*, 1365.
- (9) Song, J. E.; Kim, Y. H.; Kang, Y. S. *Curr. Appl. Phys.* **2006**, *6*, 791.
- (10) Rhodes, C.; Franzen, S.; Maria, J. P.; Losego, M.; Leonard, D. N.; Laughlin, B.; Duscher, G.; Weibel, S. *J. Appl. Phys.* **2006**, *100*, 054905.
- (11) Franzen, S. *J. Phys. Chem. C* **2008**, *112*, 6027.
- (12) Kanehara, M.; Koike, H.; Yoshinaga, T.; Teranishi, T. *J. Am. Chem. Soc.* **2009**, *131*, 17736.
- (13) Zhao, S.; Guo, Y.; Song, S.; Choi, D.; Hahn, J. *Appl. Phys. Lett.* **2012**, *101*, 053117.
- (14) Granqvist, C. G.; Hamberg, I.; Svensson, J. S. E. M. *Ind. Eng. Chem. Prod. Res. Dev.* **1985**, *24*, 93.
- (15) Gazotti, W. A.; Casalbore-Miceli, G.; Geri, A.; Berlin, A.; de Paoli, M. A. *Adv. Mater.* **1998**, *10*, 1522.
- (16) Pichot, F.; Ferrere, S.; Pitts, R. J.; Gregg, B. A. *J. Electrochem. Soc.* **1999**, *146*, 4324.
- (17) Betz, U.; Kharrazi Olsson, M.; Marthy, J.; Escolá, M. F.; Atamny, F. *Surf. Coat. Technol.* **2006**, *200*, 5751.
- (18) <http://www.agc-automotive.com/english/products/cool.html>.
- (19) Granqvist, C. G. *Sol. Energy Mater. Sol. Cells* **2007**, *91*, 1529.
- (20) Biswas, P. K.; De, A.; Pramanik, N. C.; Chakraborty, P. K.; Ortner, K.; Hock, V.; Korder, S. *Mater. Lett.* **2003**, *57*, 2326.
- (21) Alam, M. J.; Cameron, D. C. *Thin Solid Films* **2000**, *377–378*, 455.
- (22) Al-Dahoudi, N.; Aegerter, M. A. *J. Sol-Gel Sci. Technol.* **2003**, *26*, 693.
- (23) Girtan, M.; Folcher, G. *Surf. Coat. Technol.* **2003**, *172*, 242.
- (24) Ohta, H.; Orita, M.; Hirano, M.; Tanji, H.; Kawazoe, H.; Hosono, H. *Appl. Phys. Lett.* **2000**, *76*, 2740.
- (25) Bender, M.; Seelig, W.; Daube, C.; Frankenberger, H.; Ocker, B.; Stollenwerk, J. *Thin Solid Films* **1998**, *326*, 72.
- (26) Hu, Y.; Diao, X.; Wang, C.; Hao, W.; Wang, T. *Vacuum* **2004**, *75*, 183.
- (27) Miyazaki, H.; Ota, T.; Yasui, I. *Sol. Energy Mater. Sol. Cells* **2003**, *79*, 51.
- (28) Yin, Y.; Zhou, S.; Gu, G.; Wu, L. *J. Mater. Sci.* **2007**, *42*, 5959.
- (29) Chatterjee, S. *J. Mater. Sci.* **2008**, *43*, 16.
- (30) Tao, P.; Viswanath, A.; Schadler, L. S.; Benicewicz, B. C.; Siegel, R. W. *ACS Appl. Mater. Interfaces* **2011**, *3*, 3638.
- (31) Liu, H.; Zeng, X.; Kong, X.; Bian, S.; Chen, J. *Appl. Surf. Sci.* **2012**, *258*, 8564.
- (32) Saito, R.; Kuwano, K.; Tobe, T. *J. Macromol. Sci., Part A: Pure Appl. Chem.* **2002**, *39*, 171.
- (33) Kubo, T.; Tadaoka, E.; Kozuka, H. *J. Mater. Res.* **2004**, *19*, 635.
- (34) Kubo, T.; Tadaoka, E.; Kozuka, H. *J. Sol-Gel Sci. Technol.* **2004**, *31*, 257.
- (35) Kozuka, H.; Fujita, M.; Tamoto, S. *J. Sol-Gel Sci. Technol.* **2008**, *48*, 148.
- (36) Dallas, P.; Bourlinos, A. B.; Niarchos, D.; Petridis, D. *J. Mater. Sci.* **2007**, *42*, 4996.
- (37) Jin, Y.; Yi, Q.; Ren, Y.; Wang, X.; Ye, Z. *Nanoscale Res. Lett.* **2013**, *8*, 153.
- (38) Kim, S.-S.; Choi, S.-Y.; Park, C.-G.; Jin, H.-W. *Thin Solid Films* **1999**, *347*, 155.
- (39) Frank, G.; Köstlin, H. *Appl. Phys. A: Mater. Sci. Process.* **1982**, *27*, 197.
- (40) Underwood, S.; Mulvaney, P. *Langmuir* **1994**, *10*, 3427.
- (41) Shi, W.; Zeng, H.; Sahoo, Y.; Ohulchanskyy, T. Y.; Ding, Y.; Wang, Z. L.; Swihart, M.; Prasad, P. N. *Nano Lett.* **2006**, *6*, 875.
- (42) Kumon, S. In *New Technology of Sol-Gel Processing*; Sakka, S., Ed.; CMC Publishing Co. Ltd.: Tokyo, 2010; p 142.